Spin-reorientation phase transitions in yttrium-samarium iron garnets

V. A. Borodin, V. D. Doroshev, R. Z. Levitin, V. Nekvasil,[1)] V. N. Orlov, and T. N. Tarasenko

Donetsk Physicotechnical Institute, Ukrainian Academy of Sciences

(Submitted 6 December 1983)
Zh. Eksp. Teor. Fiz. **86**, 2255–2262 (June 1984)

Comprehensive magnetic and structural studies of the yttrium-samarium iron garnets $Sm_xY_{1-x}Fe_5O_{12}$ ($0.27 \leqslant x \leqslant 3$) are carried out. An orientational (x, T) phase diagram is plotted and indicates that when the temperature is lowered the sequence $\langle 111\rangle \leftrightarrow \langle 110\rangle \leftrightarrow \langle uv0\rangle$ of spin-reorientation phase transitions observed in ferrites having $x > x_{cr} \approx 0.1$ is the same as in the samarium iron garnet $Sm_3Fe_5O_{12}$, the transition temperature decreasing rapidly with increase of the diamagnetic dilution. Only easy directions of the $\langle 111\rangle$ type occur at $1.7\ \text{K} < T < T_N$ in ferrites with $x < x_{cr}$. The orientational phase diagram of the ferrites $Sm_xY_{3-x}Fe_5O_{12}$ is theoretically calculated in the crystal-field approximation. The calculation has shown that all the singularities of the diagram, as well as the observed reversal of the sign of the anisotropy constant K_2 with change of the concentration x can be attributed to the concentration dependence of only one of the nine crystal-field parameters B_{kq}, namely B_{20}.

Besides the well investigated[1-2] first-order spin-reorientation (SR) phase transition $\langle 111\rangle \leftrightarrow \langle 110\rangle$ at $T_{r2} = 66$ K in samarium iron garnet (IG) $Sm_3Fe_5O_{12}$, there was recently observed and investigated[3,4] a second-order SR at $T_{r1} = 18$–19 K. In this transition the direction of the easy magnetization rotates away from the $\langle 110\rangle$ direction in $\{100\}$ planes, so that 24 degenerate canted phases of the $\langle uv0\rangle$ type are produced in $Sm_3Fe_5O_{12}$ below T_{r1}. Both SR phase transitions were explained in Ref. 4 within the framework of a single model based on the hypothesis that the Sm^{3+} ions in the garnet structure have an Ising magnetic ordering. Recently[5] the SR diagram of $Sm_3Fe_5O_{12}$ was also described microscopically in the one-ion approximation with account taken of the crystal field and of the isotropic interaction between a rare earth and iron.

It was observed earlier[6] that in mixed yttrium-samarium IG $Sm_xY_{3-x}Fe_5O_{12}$ the temperature T_{r2} of the $\langle 111\rangle \leftrightarrow \langle 110\rangle$ SR transition shifts towards lower temperatures with increasing yttrium content, and that this transition does not occur in compositions with $x \leqslant 1.05$. The low-temperature SR transitions $\langle 110\rangle \leftrightarrow \langle uv0\rangle$ in mixed yttrium-samarium IG have not been investigated before.

We report here comprehensive magnetic, magneto-optical, and structural investigations of single-crystal samples of yttrium-samarium IG $Sm_xY_{3-x}Fe_5O_{12}$ ($x = 0.27$; 0.51; 1.05; 1.57; 2.17; 2.5; 3), aimed at constructing the magnetic SR phase diagram of these ferrimagnets.

The spin-reorientation temperatures T_{r1} and T_{r2} were determined from the maxima on the temperature dependence of the initial magnetic susceptibility (the measurements were made at the frequencies 220 Hz and 20 kHz) and from the torque curves. The torque method was used also to determine the orientation of the easy magnetization axis (EMA). The measurements were made in the temperature range 1.7–77 K.

To determine the character of the low-temperature SR transition we investigated by x-ray diffraction the crystal structure of $Sm_3Fe_5O_{12}$ in the temperature interval 5.5–30 K. In addition, in the interval 4.2–80 K we measured the magnetization, the magnetostriction, and the Faraday effect in pulsed magnetic fields up to 270 kOe along the crystallographic axes $\langle 111\rangle$, $\langle 110\rangle$, and $\langle 100\rangle$, and were thus able to determine the saturation fields along these directions. The procedures employed are described in Refs. 7–12.

The measurements were made on $Sm_xY_{3-x}Fe_5O_{12}$ single crystals grown by crystallization from the molten solution. The samples were oriented by the x-ray and and magnetic methods accurate to 1–3°. Figure 1 shows the (x, T) phase diagram of the IG $Sm_xY_{3-x}Fe_5O_{12}$, obtained from our measurements in a zero magnetic field. At high temperatures, in the entire range $0 \leqslant x \leqslant 3$, there were realized $\langle 111\rangle$ phases in which the easy magnetization directions coincided with axes of the $\langle 111\rangle$ type.

Lowering the temperature leads, in compositions with large samarium contents, to a first order SR transition $\langle 111\rangle \leftrightarrow \langle 110\rangle$, where the directions of the easy magnetization are now axes of the $\langle 110\rangle$ type. The temperature T_{r2} of the SR transition decreases with decreasing samarium content, and this transition is not observed at $x \lesssim 1.05$. Our values of T_{r2} agree well with the data of Ref. 6.

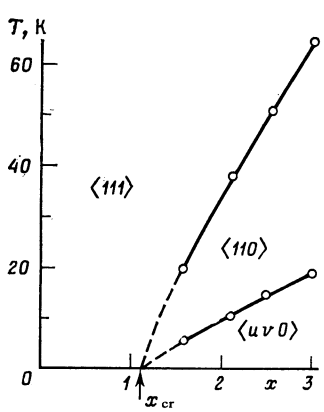

FIG. 1. Experimental spin-reorientation phase diagram of iron garnets of the $Sm_xY_{3-x}Fe_5O_{12}$ system. The temperatures $T_{r1}(x)$ and $T_{r2}(x)$ of the spontaneous phase transitions were determined from the maxima of the initial magnetic susceptibility. The phase-transition lines for $x < 1.57$ are extrapolated.

 0038-5646/84/061312-04$04.00

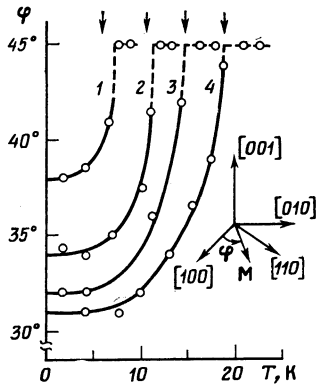

FIG. 2. Temperature dependence of the angle φ that determines the orientation of the magnetization vector **M** in the canted phases $\langle uv0\rangle$ of iron garnets of the $Sm_xY_{3-x}Fe_5O_{12}$ system at various samarium concentrations: 1—$x = 1.57$; 2—2.1; 3—2.5; 4—3. The data were obtained by the torque method. The arrows indicate the transition temperatures T_{r1} determined from the maxima of the initial magnetic susceptibility.

With further lowering of the temperature, in compositions with $x \geqslant 1.57$, a second SR transition of type $\langle 110\rangle \leftrightarrow \langle uv0\rangle$ is observed: at the temperature T_{r1} the easy-magnetization direction is rotated away from the $\langle 110\rangle$ axes in the $\{100\}$ planes. The orientation of the magnetization in the $\langle uv0\rangle$ phases can be characterized by the angle $\varphi(T)$ between the magnetization vector and the $\langle 100\rangle$ axis. As seen from Fig. 2, this angle is 45° in the $\langle 110\rangle$ phase and decreases smoothly as the temperature drops below T_{r1}, but the angle φ is not equal to zero at 0 K.

The conclusion that a transition from the $\langle 110\rangle$ to the $\langle uv0\rangle$ phase takes place in $Sm_3Fe_5O_{12}$ at low temperatures is confirmed by x-ray measurements. It follows from symmetry considerations that owing to the magnetoelastic strains the cubic crystal structure of $Sm_3Fe_5O_{12}$ and of mixed yttrium–samarium IG should become distorted. These distortions are rhombohedral (space group $R\bar{3}m$) in the $\langle 111\rangle$ phase, rhombic (space group $Immm$) in the $\langle 110\rangle$ phase), and monoclinic (space group $C2/m$) in the $\langle uv0\rangle$ phase. X-ray measurements have shown that in $Sm_3Fe_5O_{12}$ the type of the cubic-crystal structure distortions changes below 20 K from rhombic to monoclinic. The monoclinic distortions increase smoothly as the temperature is decreased to below the SR transition point. This, as well as the aforementioned smooth variation of the angle φ with temperature (see Fig. 2), indicates that the $\langle 110\rangle \leftrightarrow \langle uv0\rangle$ phase transition is of second order.[2)]

The SR phase transition $\langle 110\rangle \leftrightarrow \langle uv0\rangle$, as well as the transition $\langle 111\rangle \leftrightarrow \langle 110\rangle$, is not observed in samples having $x \leqslant 1.05$. Extrapolation of the line of the this transition on Fig. 1 to $T = 0$ K shows that the critical density concentration x_{cr} of the samarium is 1.1. The value of x_{cr} was determined by us approximately, and to refine it, as well as to reveal the singularities of the phase diagram near x_{cr}, investigations of the compositions near the critical concentrations are necessary. These investigations can show whether the transitions $\langle 111\rangle \leftrightarrow \langle 110\rangle$ and $\langle 110\rangle \leftrightarrow \langle uv0\rangle$ vanish at the same concentration or whether there exists a range of compositions in which the transition $\langle 111\rangle \leftrightarrow \langle uv0\rangle$ is realized (see below).

It can be seen from Fig. 2 that the limiting, extrapolated to 0 K, angle of deviation of the easy-magnetization direction decreases with increasing samarium content, from φ (0 K) = 38° to φ (0 K) = 31° at $x = 3$. The dependence of φ(0 K) on the concentration x will also permit z_{cr} to be determined by extrapolation to $\varphi = 45°$. The value of x_{cr} determined in this manner is in the range 1.1–1.3.

The saturation fields of the IG $Sm_xY_{3-x}Fe_5O_{12}$ along the crystallographic directions $\langle 111\rangle$, $\langle 110\rangle$, and $\langle 100\rangle$ were measured in that temperature interval in which these directions are not EMA. It was observed that they increase rapidly with decreasing temperature, and we were able to achieve saturation in fields up to 270 kOe for compositions with $x \geqslant 2.5$ at $T \leqslant T_{r2}$.

The magnetic anisotropy constants K_1 and K_2 were determined from the experimental values of the saturation fields by means of formulas given, e.g., in Ref. 13. Figure 3 shows the values of K_1 and K_2 as functions of the temperature. It can be seem from this figure that when the temperature is lowered the absolute values of K_1 and K_2 increases steeply. $K_1 < 0$ for all the investigated concentrations, while K_2 reverses sign near $x \approx 1.5$ (Fig. 3). This phenomenon was observed earlier[14] at higher temperatures. We note that the cited values of K_1 and K_2 at low temperatures ($T \approx T_{r2}$) must be regarded only as effective ones. The reason is that they

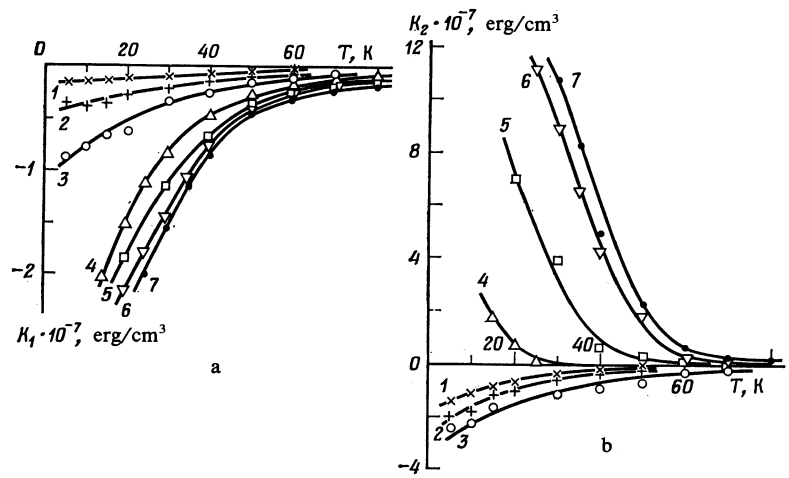

FIG. 3. Temperature dependences of the anisotropy constants K_1 and K_2 (b) of iron garnets of the $Sm_xY_{3-x}Fe_5O_{12}$ system at different Sm concentrations: 1—$x = 0.27$; 2—0.51; 3—1.05; 4—1.57; 5—2.10; 6—2.5; 7—3.

were calculated in an approximation with two anisotropy constants, whereas, as shown in Ref. 13, the transition $\langle 110\rangle \leftrightarrow \langle uv0\rangle$ can be described phenomenologically only by taking into account, in the magnetic-anisotropy energy, interactions of eight order in the direction cosines of the magnetization vector (third magnetic-anisotropy constant), and this interaction should be appreciable ($K_1<0$; K_2, $K_3>0$; $K_1/K_3 \geqslant -0.5$; $K_2/K_3 \geqslant 2$). Moreover, it was noted in Ref. 4 that for most rare-earth IG it is incorrect to represent the magnetic-anisotropy energy as an additive part of the free energy, for in these ferrimagnets the isotropic exchange interaction between the rare-earth (RE) ions and the iron ions is weaker than their interaction with lattice crystal field that determines the magnetic anisotropy. For example, the model with Ising ordering of the Sm^{3+} ions, proposed in Ref. 4 to describe the SR transitions in the IG $Sm_3Fe_5O_{12}$, admits of separation of the one-ion magnetic-anisotropy energy as an additive increment to the exchange energy only under the condition $\mu_{Sm}H_{mol}/kT \ll 1$ (H_{mol} is the molecular field acting on the rare-earth sublattice), i.e., at temperatures on the order of 10–100 K.

In the theoretical description of the properties of the samarium IG, both in the Ising approximation[4] and in the microscopic treatment,[5] two mechanisms were taken into account: the RE–iron isotropic exchange and the one-ion anisotropic interaction of the rare earth with the crystal lattice field. Both interactions are proportional to the number of Sm^{3+} ions, i.e., they are independent of the concentration when referred to one ion in the mixed IG $Sm_xY_{3-x}Fe_5O_{12}$. Therefore, it it is assumed that the exchange interaction and the crystal-field parameters in $Sm_xY_{3-x}Fe_5O_{12}$ do not change when the samarium is replaced by yttrium, the energy (per Sm^{3+} ion) is independent of the samarium constant, so that the temperatrues T_{r1} and T_{r2} of the SR transitions should be independent of the samarium concentration (at any rate up to concentrations at which the anisotropy of the iron sublattice becomes comparable with that of the diluted samarium sublattice, $x \sim 0.01$.

To explain the strong samarium-concentration dependence of the temperatures T_{r1} and T_{r2} observed experimentally in $Sm_xY_{3-x}Fe_5O_{12}$ it is necessary to take into account the concentration dependence of the crystal-field parameters. The RE ion in the garnet structure is in a dodecahedral surround of O^{2-} ions, and the crystal field acting on this ion is determined by the parameters of this dodecahedron. When one RE ion is replaced by another (or by yttrium) having a different ion radius, the surround is deformed so that the crystal-field parameter is changed. There is practically no information in the literature on how the parameter of the crystal field acting on the rare-earth ion changes on going from one matrix with garnet structure to another. The data of Ref. 15 for Nd^{3+} in various garnets show that out of the nine crystal-field parameters B_{kq} the most strongly dependent on the matrix is B_{20}: on going from one paramagnetic garnet to another this parameter changes not only in magnitude but also in sign. We have assumed that a similar phenomenon occurs also in $Sm_xY_{3-x}Fe_5O_{12}$ garnets, viz., the parameters B_{kq} change with changing samarium concentration, and calculated the changes of the samarium IG properties with changing B_{20}.

The Hamiltonian of the Sm^{3+} ion was chosen in the form

$$\mathcal{H} = \sum_{kq} B_{kq}C_q^k + g_s\mu_B H_{ex}S. \qquad (1)$$

The first term describes the interaction with the crystal field (B_{kq} are the crystal-field parameters, C_q^k are irreducible tensor operators expressed in terms of combinations of spherical harmonics[16]) and the second describes the interaction of the spin S of the Sm^{3+} ion with the isotropic exchange field H_{ex} due to surrounding iron ions. Starting from the Hamiltonian (1) we calculated the wave functions and energy levels of Sm^{3+} with account taken of the three lower multiplets $^4F_{5/2}$, $^4F_{7/2}$, and $^4F_{9/2}$. From these we determined next the free energy of the garnet at various temperatures (summing in this case over the six nonequivalent positions of the RE ions in the garnet structure). The calculations were performed for different orientations of H_{ex} in the crystal, and the direction for which the free energy is a minimum (the EMA) was found. The calculation procedure is described in greater detail in Ref. 5. In the calculation we varied the crystal-field parameter B_{20} and chose the remaining B_{kq} and H_{ex} to be equal to those used to describe the phase diagram of the IG $Sm_3Fe_5O_{12}$ in Ref. 5, viz., $B_{22}=181$, $B_{40}=-2250$, $B_{42}=242$, $B_{44}=1009$, $B_{60}=870$, $B_{62}=-171$, $B_{64}=1297$, $B_{66}=-170\ cm^{-1}$, $\mu_B H_{ex}/k = 29$ K.

Figure 4 shows the variation of the magnetic phase diagram with changing B_{20}. It can be seen that when $|B_{20}|$ decreases from the value of $Sm_3Fe_5O_{12}$ ($B_{20}=-171\ cm^{-1}$) the temperatures T_{r1} of the $\langle 111\rangle \leftrightarrow \langle 110\rangle$ transitions and T_{r2} of the $\langle 110\rangle \leftrightarrow \langle uv0\rangle$ transitions decrease and at $|B_{20}| \leqslant 97\ cm^{-1}$ the phase that is stable in the entire temperature range is $\langle 111\rangle$. This phase diagram is qualitatively similar to the experimental phase diagram of $Sm_xY_{3-x}Fe_5O_{12}$ (see Fig. 1). To compare them it is necessary only to assume that B_{20} depends linearly on the samarium concentration in $Sm_xY_{3-x}Fe_5O_{12}$ (the upper abscissa scale of Fig. 4). Theoretical calculations show that in the model considered the

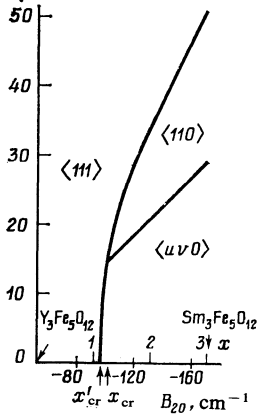

FIG. 4. Theoretical spin-reorientation phase diagram of iron garnets of the system $Sm_xY_{3-x}Fe_5O_{12}$.

anisotropy constant K_2 reverses sign near the critical concentration x_{cr}; this also agrees with the experimental data (see Fig. 3).

The theoretical analysis has thus confirmed the hypothesis that the variation of the properties of $Sm_xY_{3-x}Fe_5O_{12}$ with changing concentration is due to changes of the crystal-field parameters. Moreover, our estimates show that the principal role is played by the change of the crystal-field parameter B_{20}, while the changes of the other parameters affect the properties much less. From our viewpoint this is most important, since we have succeeded in identifying the most important of the nine parameters B_{kq}, namely B_{20}, which determines in fact the evolution of the properties of $Sm_xY_{3-x}Fe_5O_{12}$.

We emphasize that at present there is no theory capable of connecting the change of the parameter B_{20} with the change of the $Sm_xY_{3-x}Fe_5O_{12}$ crystal structure. In this sense, too, the foregoing theoretical treatment is semi-empirical. It can only be stated that replacement of the Sm^{3+} ions, which have a large ion radius,[3)] with Y^{3+} ions with relatively small radius can alter greatly the parameters of the dodecahedral surround and hence change B_{kq} significantly.

We note that near the critical concentration x_{cr} there is a certain qualitative difference between the theoretical and experimental phase diagrams: the theoretical diagram is shifted upward, as it were, so that the line of the first-order $\langle 111\rangle \leftrightarrow \langle uv0\rangle$ SR transition appear, with $x'_{cr} \approx 1.05$. This transition cannot occur in a phenomenological treatment with allowance for the three anisotropy constants K_1, K_2, and K_3 (Ref. 13). Better agreement can apparently be reached by varying somewhat the calculation parameters (say, the value of the exchange). It seems to us, however, that this is unnecessary, since the model is a crude one. In particular, it neglects the important fact that mixed yttrium-samarium IG cannot be regarded as homogeneous systems: the parameters of the dodecahedral surround at the places occupied by samarium differ from those at the places occupied by yttrium. In addition, no account in taken in the calculation of the anisotropic RE–iron exchange. This may explain why the theoretical limiting angles $\varphi(0\ \mathrm{K})$ for all $x > 1.2$ change insignificantly (by 1–2 deg), whereas experiment shows them to decrease by 7° when x is increased from 1.57 to 3.

In conclusion, we compare the $Sm_3Fe_5O_{12}$ properties calculated in Ref. 5 with the hypothesis of Ising ordering in this ferrimagnet, proposed in Ref. 4. According to this hypothesis the energy ground state of the Sm^{3+} ion in the crystal field is a doublet greatly separated in energy from the lower-lying levels, and the wave functions of this doublet are such that only one x component of the g tensor differs from zero. A calculation of the energy levels and of the g factors of Sm^{3+} using the crystal-field parameters of Ref. 5 has shown that the g factors of the ground doublet of Sm^{3+} in the garnet are $g_x = 0.842$, $g_y = 0.013$, $g_z = 0.075$, i.e., $g_x \gg g_y, g_z$. The hypothesis that the Sm^{3+} ions in the Sm IG have an Ising order is consequently confirmed by the microscopic calculation in the crystal-field approximation.

The authors thank K. P. Belov and N. M. Kovtun for a discussion of the results and for constant interest in the work, and thank also G. A. Babushkin, A. K. Zvezdin, and A. I. Poov for helpful discussions.

[1)]Physics Institute, Czechoslovak Academy of Sciences, Prague.

[2)]This conclusion, naturally is restricted by the measurement accuracy. According to our data it can be stated that the jump of the angle φ in the SR transition is at any rate less than 1°.

[3)] Of all the rare-earth ions, Sm^{3+} has the largest radius that permits formation of a pure IG: Pr^{3+} and Nd^{3+} have larger radii but form only partially substituted IG.

[1]F. W. Harrison, J. F. A. Thompson, and G. K. Lang, J. Appl. Phys. **36**, 1014 (1965).
[2]V. A. Borodin, V. D. Doroshev, V. A. Lkochan, *et al.*, Fiz. Tverd. Tela (Leningrad) **18**, 1852 (1976) [Sov. Phys. Solid State **18**, 1080 (1976)].
[3]S. Geller and G. Balestrina, Phys. Rev. **B21**, 4055 (1980).
[4]G. A. Babushkin, V. A. Borodin, V. D. Doroshev, *et al.*, Pis'ma Zh. Eksp. Teor. Fiz. **35**, 28 (1982) [JETP Lett. **35**, 34 (1982)].
[5]N. Guillot, A. Marchand, V. Nekvasil, and F. Tcheou, J. Phys. C, 1984, in press.
[6]N. M. Kolachev, N. M. Kolacheva, R. Z. Levitin, *et al.*, State **19**, 359 1(977)].
[7]V. G. Bar'yakhtar, V. A. Borodin, V. D. Doroshev, *et al.*, Zh. Eksp. Teor. Fiz. **74**, 600 (1978) [Sov. Phys. JETP **47**, 315 (1978)].
[8]V. A. Borodin, V. D. Doroshev, and T. N. Tarasenko, VINITI deposited paper No. 669-81, 12 February 1981.
[9]R. Z. Levint, A. S. Markosyan, and V. N. Orlov, Fiz. Tverd. Tela (Leningrad) **25**, 1861 (1983) [Sov. Phys. Solid State **25**, 1074 (1983).
[10]I. S. Jacobs and P. E. Lawrence, Rev. Sci. Inst. **29**, 713 (1958).
[11]A. K. Zvezdin, R. Z. Levitin, A. I. Popov, and V. I. Silant'ev, Zh. Eksp. Teor. Fiz. **80**, 1504 (1981) [Sov. Phys. JETP **53**, 771 (1981)].
[12]U. V. Valiev, R. Z. Levitin, K. M. Mukimov, *et al.*, Fiz. Tverd. Tela (Leningrad) **23**, 2182 (1981) [Sov. Phys. Solid State **23**, 1278 (1981)].
[13]K. P. Belov, A. K. Zvezdin, A. M. Kadomtseva, and R. Z. Levitin, Orientatsionnye perekhody v redkozemel'nykh magnetikakh (Orientational Transitions in Rare-Earth Magnets), Nauka, 1979.
[14]N. M. Kolacheva, R. z. Levitin, and L. P. Shlyakina, Fiz. Tverd. Tela (Leningrad) **19**, 970 (1977) [Sov. Phys. Solid State **19**, 565 (1977)].
[15]V. Nekvasil, Phys. Stat. Sol. (b). **87**, 317 (1978).
[16]D. J. Newman, Adv. Phys. **20**, 197 (1971).

Translated by J. G. Adashko